Adsorption Behavior of 5Fluorouracil on Au(111): An In Situ STM Study

ARTICLE *in* THE JOURNAL OF PHYSICAL CHEMISTRY C · APRIL 2010

Impact Factor: 4.77 · DOI: 10.1021/jp100890a

4 AUTHORS, INCLUDING:

Hilton Barbosa de Aguiar
Institut Fresnel
22 PUBLICATIONS **305** CITATIONS
SEE PROFILE

Frederico Cunha
Universidade Federal de Sergipe
23 PUBLICATIONS **418** CITATIONS
SEE PROFILE

Adsorption Behavior of 5-Fluorouracil on Au(111): An In Situ STM Study

H. B. de Aguiar,[†,‡] F. G. C. Cunha,[§] F. C. Nart,[∥,⊥] and P. B. Miranda*[,‡]

Instituto de Física de São Carlos and Instituto de Química de São Carlos, Universidade de São Paulo, CP 369, São Carlos, São Paulo, Brazil 13560-970, and Departamento de Física, Universidade Federal de Sergipe, CP 353, São Cristóvão, Sergipe, Brazil 49100-000

Received: January 29, 2010; Revised Manuscript Received: February 25, 2010

The biological effects of chemical substitution of DNA bases triggered several investigations of their physicochemical properties. This paper studies the adsorption behavior of a halogenated uracil, 5-fluorouracil (5FU), at the electrochemical interface of Au(111) and sulfuric acid solution. Upon modulation of the electric field across the interface, four distinct phases could be inferred by means of cyclic voltammetry (CV). At negative potentials relative to the SCE electrode, limited by the threshold of hydrogen evolution, no molecular species could be detected by scanning tunneling microscopy (STM) at the reconstructed Au(111)-$(23 \times \sqrt{3})$ surface, indicating that any physisorbed molecules are randomly distributed. Incursion into more positive potentials increases the surface population but *does not* form any two-dimensional (2D) physisorbed ordered structure. Instead, we observed metastable structures that are only detectable on surfaces with high defect density. At sufficiently high positive potentials, limited by gold oxidation, the molecules are chemisorbed in a $(3 \times 2\sqrt{3})$ ordered structure, with the aromatic ring perpendicular to the surface. We report the densest chemisorbed monolayer for pyrimidine-derivative molecules (area per molecule 0.14 ± 0.04 nm^2). A comparison of the adsorption behavior of uracil derivatives has been made based on recent results of chemical substitution and solvent effects. We propose that π-stacking is enhanced when halogens are incorporated in the uracil structure, in a similar fashion to what is observed in their crystal structure.

Introduction

Studies concerning uracil and its derivatives have been performed by several authors to determine the effects of chemical substitution on real biological systems. To determine the physicochemical structures of such compounds, several aspects have been investigated, including electronic structure,[1] absorption and emission spectra,[2,3] hydrogen-bonding and intermolecular vibrations,[4] tautomerism,[5,6] acidities, proton affinities, and base pairing energies.[7] Among these studies, two main classes of uracil derivatives can be identified: halogen and sulfur-containing. Such investigations were triggered by the mutagenic effects of uracil derivatives upon incorporation into DNA or RNA. For instance, it has been hypothesized that incorporation of halogen uracil (replacing Thymine) in DNA leads to a preferential base pairing with guanine, instead of adenine, disrupting the genetic code.[8] This and other substitution effects have turned 5-fluorouracil (5FU) into one of the most successful chemotherapy agents in colorectal cancer treatment.[9]

The adsorption of uracil and its derivatives onto solid surfaces has been studied not only for the sake of understanding its physical and chemical properties[10] but also for its possible application in drug-delivery systems, using for example metal nanoparticles as a drug-carrying medium.[11] Another motivation for adsorption studies of uracil derivatives is the ability of nucleic acids to form different patterns of hydrogen bonds from base to base.[12,13] In the very beginning of these studies, the majority were done at the electrified mercury/solution interface.[14] Many uracil derivatives were extensively studied and some other nucleic acids as well.[15] In general, for the case of mercury substrates, adsorption occurs as physisorption. Variation of the external parameters, such as electric field across the interface, bulk concentration, pH, or temperature, leads to different states of adsorption. In these studies, it was proposed that molecules change from randomly physisorbed and flat-lying to a condensed upstanding state.[16] Later on, it was suggested that this condensed phase in fact forms flat-lying periodic structure similar to their crystal structure,[17] not a condensed upstanding phase. This research area has flourished once again since new techniques for growing solid single-crystal and probes with atomic/molecular resolution were developed.[18] Different states of adsorption were achieved depending on molecular structure,[19] substrate,[20] and crystallographic orientation.[21] Adsorption at MoS_2,[12] graphite,[22] Au,[23] Ag,[24] and Cu[25] substrates were imaged with molecular resolution in electrified environment and spontaneously adsorbed. Recently, coadsorption of complementary bases opened a new branch in this area of research.[12,26−29]

The study of organic adsorbates is divided in several areas but two of them received special attention: sulfur-containing (e.g., alkyl thiols) and nitrogen-containing (e.g., pyridine) molecules. In the first case, the monolayer formation through a self-assembling mechanism has a very strong chemical bond between the sulfur atom and the metal surface forming a stable and usually organized adlayer.[30] For nitrogen-containing molecules adsorbed on group IB metals a more versatile behavior is observed.[31] In the particular cases of gold and silver, the careful control of the surface charge may lead to changes in the adsorption state of these molecules.[32]

A less-studied class of adsorbates are the halogen-containing molecules, with most studies focused on chemical reactions of

* Corresponding author. E-mail: miranda@ifsc.usp.br.
† Current address: Max-Planck-Institute für Metallforschung, Heisenbergstrasse 3, 70569, Stuttgart, Germany.
‡ Instituto de Física de São Carlos, Universidade de São Paulo.
§ Universidade Federal de Sergipe.
∥ Instituto de Química de São Carlos, Universidade de São Paulo.
⊥ Deceased. We dedicate this work to his memory.

10.1021/jp100890a
Published on Web 03/10/2010

adsorbates[33−35] and, surprisingly enough, only a few for the electrochemical interfaces.[16,36,37] These studies comparing the so-called halo-uracil molecules show drastically distinct behaviors, for example, 5-iodoracil (5IU) upon adsorption on Ag(111) reacts with another 5IU forming a new molecular structure, but 5-clorouracil (5ClU) physisorbs up to three layers on the same surface.[38] So, it is suggestive that the presence of different halogens in the pyrimidine ring opens up new behaviors clearly distinct from the ones reported for methyl- or sulfur-substituted uracil. The purpose of this paper is to address the adsorption behavior of 5FU on single crystalline gold and compare it to other uracil derivatives.

In this study we map out the adsorption behavior of 5FU at the Au(111) electrified interface. Because 5FU and uracil have similar chemical structure, it is suggestive to compare the adsorbed states of both molecules. Wandlowski and collaborators, in a series of communications, have convincingly and thoroughly described this latter system.[17,19−21,37,39,40] To aid the presentation and discussion of our results, we want to briefly review the assignments of the adsorbed phases of uracil (the "simplest" molecular structure) on Au(111).[19,39] There are four distinct phases labeled I, II, III, and IV. Phase I is at relatively high negative potentials, limited by hydrogen evolution, and the uracil molecules are randomly adsorbed (gas-like), coadsorbed with water molecules. Further potential increase leads to phase II, characterized by a spike in the cyclic voltammogram (CV), indicating a first-order phase transition. In this state, STM images show that uracil molecules are flat-lying physisorbed forming a 2D periodic structure stabilized by hydrogen bonds in good agreement with crystallographic data.[39] Crossing the potential of zero charge leads to phase III characterized in the CV by a large charge transfer which involves a mix of reorientation of the molecular ring, deprotonation and substrate reconstruction lifting. Higher positive potentials, limited by Au reversible oxide formation, leads to a new peak in the CV assigned to phase IV. In this phase, a close-packed chemisorbed periodic structure is formed and the molecular rings are in an upright orientation.

Experimental Section

All solutions were prepared with ultrapure water (Millipore system), H_2SO_4 (Merck, suprapure), and 5FU (Fluka, puriss). The latter was used as received. The solutions were not stocked.

Three different Au(111) electrodes were used: a small bead and disks. A bead obtained by melting a gold wire is used only for CV results since it has lower defect density. The disks were purchased from Metal Crystal and Oxides (Cambridge, U.K., 10 mm diameter, 3 mm height) and Surface Preparation Laboratory (The Netherlands, 12 mm diameter, 3 mm height). Before each experiment, the electrodes were flame-annealed to red heat with H_2/O_2 and cooled in a N_2 or an Ar atmosphere for ~4 min. Transfers to respective systems (CV and STM) were done with a water droplet protecting the surface. Contact with electrolyte was established under strict potential control (−100 mV/SCE). To check the quality of the electrodes CV of pure electrolytes were done. The profile of the reconstruction lifting and the peak of formation of a condensed sulfate adlayer are indicators.[40]

All electrochemical (CV) experiments were carried in a conventional three-electrode system, recorded with a potentiostat Autolab PGSTAT30 (Eco Chemie). Hanging meniscus configuration was used to isolate only the surface of interest. The counter electrode was a Pt foil flame-annealed before experiment. The reference electrode was a reversible hydrogen electrode (RHE), but all CVs are quoted with respect to the saturated calomel electrode (SCE).

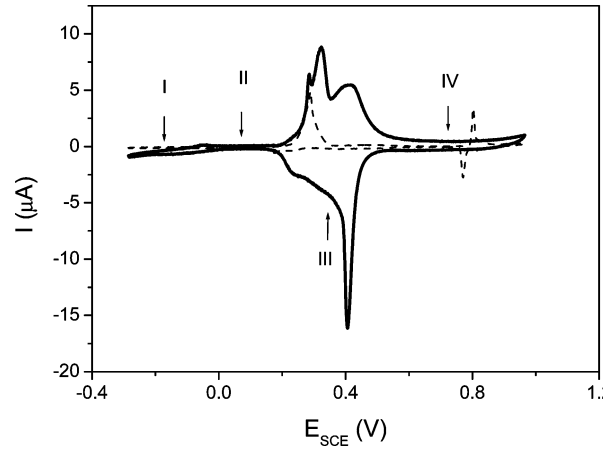

Figure 1. Steady state cyclic voltammogram of 6 mM 5FU/50 mM H_2SO_4/Au (111); scan rate, 50 mV s^{-1}. The dashed lines is a 5FU-free solution (only electrolyte).

In situ STM imaging was performed either with a PicoSPM (Molecular Imaging, Tempe, EUA) or Topometrix Discoverer 2010, both equipped with bipotentiostats. The tungsten tips (0,25 mm diameter) were electrochemically etched in NaOH (2 M) solutions and subsequently coated with Apiezon wax or polyethylene and then dipped for a few seconds in red nail polish (current leakage <1 pA). A platinum wire was used as counter and quasi-reference electrodes. Images are in constant current mode, otherwise stated, with a proper gray scale chosen to improve contrast.

The cell cleaning procedure has been described elsewhere.[36]

Results and Discussion

General Overview of CV. Figure 1 presents a steady-state CV with 6 mM 5FU + 50 mM H_2SO_4 on Au(111). As outlined in the Introduction, the labels I, II, III, and IV refer to adsorbed states of uracil and some of its derivatives. We could not detect a sharp current peak, indicating a first-order phase transition between phases I and II, but just a broad feature circa −40 mV/SCE. Further potential increase leads to a sharp current peak centered at 280 mV/SCE superimposed on two broader ones at 320 mV/SCE and 410 mV/SCE. Despite the absence of sharp peak indicative of I↔II phase transition, the CV of 5FU seems similar to uracil and thymine systems, namely, a small hysteresis when the potential is reversed and the number or peaks between phases II and IV, though a somewhat different relative intensity and width.[39,48] A thorough study and definitive assignment of the phases based on CV experiments is not the focus of the present work and the CV only serve to map the potentials limits of the phases. However, as we will see in the STM images, there are many similarities between 5FU and uracil, justifying the tentative assignment of the phases based on previous studies of uracil derivatives. We assign the peak at 280 mV/SCE to transition between phases II and III and the peak at 410 mV/SCE to transition between III and IV. It is worth noting that the potential of the broad and low current response (transition I↔II) was concentration-dependent (not shown), suggesting a physisorbed condensed phase transition.[21] Even at the highest bulk concentration (up to 36 mM) no sharp current peak in the CV could be resolved (transition I↔II).

One could speculate that the barely detectable I↔II transition would be due to our crystal being defect-rich, because the formation of 2D ordered physisorbed films is sensitive to the

crystal surface quality.[41] To rule this out, we show in Figure 1 (dashed lines) the CV without the 5FU, because the adsorption behavior of sulfate on Au(111) is relatively well understood and is a good indication of the quality of the single crystal.[42] The current peak between phases II and III is due to the reconstruction lifting (see In Situ STM Images). The sharp peak ~800 mV/SCE is due to a disorder/order sulfate adlayer phase transition. The detection by CV of this peak is sensitive to the quality of the crystal.[42] Its presence and strength are indications of wide Au(111) terraces, supporting the comparison between in situ STM images and CV.

Recent results reported from Pronkin and Wandlowski show that the peaks corresponding to transitions I↔II, II↔III, and III↔IV are dependent on the amount of surface defects or, in other words, how large is the Au(111) terrace.[43] These results (with and without 5FU) indicate that this single crystal has low defect density, but even so, the I↔II transition could not be resolved in CV measurements.

It is well accepted that the physisorbed phase can be distinguished into a condensed and gas-like phase (phases II and I, respectively). The first-order transition between the two phases takes place normally via a nucleation and growth kinetics causing a peak pair in the CV (e.g., uracil, thymine). In this sense only one phase is noncondensed and the other one is condensed. Results reported for the mercury electrode suggest that 5FU physisorbs; however, no information had been presented, specifying whether it was phase I or phase II (gas-like or condensed, respectively).[16,44] The only quantitative data obtained indicates that uracil molecules occupies a smaller area than 5FU in the physisorbed phase.[16]

In Situ STM Images. To follow these transitions, we have performed in situ STM experiments. First we present intermediate/high resolution images and thereafter a potentiodynamic study. Despite the CV results, we want to address two distinct behaviors for the physisorption of 5FU: on a surface with high defect density (step edges and kinks) and on another one with lower defect density (large flat terraces).

Figure 2 shows a series of images taken at different substrate potentials going from phase I to phase IV. Figure 2a is taken at phase I (−100 mV/SCE) and shows the Au(111) reconstruction characterized by the corrugation lines with periodicity of 6.3 nm.[45] Further increase in surface potential leads to phase II (100 mV/SCE) depicted in Figure 2b, but *only* the Au(111)-(23 × $\sqrt{3}$) reconstruction could be resolved. However, a pronounced increase in the noise probed by the scanning tip indicates a higher molecular population. Nevertheless, this population is not large enough to establish an ordered adlayer with long-range order. As a consequence, the molecular film cannot be imaged by STM, even at pico-amp tunneling regime. Higher resolution images (see Supporting Information) did not show any pattern like those observed for uracil[39] and thymine[46,47] in phase II, although the substrate lattice could be resolved (atomic resolution). These experiments were reproducible even at the lowest tunneling current levels allowed by the system (down to tenths of pA), but these led to higher noise levels, making images harder to take. We shall show below that the presence of topographical features stabilize these films, allowing for their imaging.

Phase III was not possible to image at higher resolution, probably due to high mobility or high disorder of the molecules and gold atoms on the surface.[43] In phase III, reconstruction is lifted expelling atoms, which form monatomic-height islands (bright spots), as shown in Figure 2c. These islands are stabilized by adsorption of 5FU molecules, which prevent growth to larger islands or be reabsorbed by defects, such as step edges and kinks. It is interesting to note similar behavior when compared to what is observed for Uracil.[39] This "rough" surface is harder to image at higher resolution, even in phase IV, where is expected to form chemisorbed periodic structures. To obtain higher resolution, we used a methodology described by Dretskow et al.[39] First, the system is set up with the electrolyte (without 5FU) in the potential of phase I, then the surface potential is swept at a rate of 10 mV s^{-1} until a potential typical of phase IV is reached. Reconstruction is lifted, but now the atoms can be reabsorbed by the surface, and Ostwald ripening allows the formation of a smooth unreconstructed surface, lowering the monatomic-height island density. At this stage, 5FU solution is added with a proper concentration and volume in order to obtain the same 6 mM 5FU concentration.

Following this procedure, phase IV (800 mV/SCE) could be imaged with molecular resolution, as presented in Figure 2d. The abrupt change in the lower part (about 1/3 of the image) is due to modifications in tip morphology, but other regions gave the same structure (with both STM setups), even within the "rough" surface. The contrast and resolution was better at this surface potential. We will assume, for now, that each blob is a single 5FU molecule. At first sight, a hexagonal close-packed structure is formed, but once the intermolecular distances in each direction are measured, they are shorter in one direction (0.33 ± 0.03 nm) than in the other two (0.45 ± 0.04 nm). This suggests that *along one row* (S1, shorter) the geometry of the molecules with respect to each other *is different from that of the other two rows* (S2, larger). For the case of uracil and thymine adsorbed on Au(111) the molecules are in a hexagonal close-packed arrangement and rotated with respect to each other.[48] Here we propose the same packing structure, but the S1 direction is smaller than those reported for similar systems.[36,39,48] The interlayer space in the solid 5FU crystal structure[49] has the value of 0.34 nm, which is in accordance with our results, demonstrating it should correspond to a real intermolecular distance. The rectangular unit cell is depicted in Figure 2d with $a = 1.02 \pm 0.03$ nm, $b = 0.85 \pm 0.03$ nm, and has (3 × 2$\sqrt{3}$) adstructure, containing six molecules. It corresponds to an area per molecule of 0.14 ± 0.04 nm^2, translating into a surface excess of 1.2×10^{-9} mol cm^{-2}. To our knowledge, this is the highest value reported in literature for pyrimidine systems. It is interesting to note that in the solid 5FU crystal structure[49] each 5FU molecule within a layer occupies the same area (for a projection perpendicular to the layer plane) as in the phase IV adlayer.

Potentiodynamic Behavior. Now we turn our attention to mesoscopic aspects of 5FU adsorption. Figure 3 presents a series of images acquired at constant-height mode of an area covered by steps edges. Constant-current images were acquired simultaneously, but the contrast was better in the former ones. The feature common to all images of Figure 3 is in the form of well-defined diagonal lines due to the atomic step edges. The experiment starts in phase I (−150 mV/SCE). In Figure 3a (at the transition between phases I and II, − 40 mV/SCE), the lack of features as well as the noise both suggest that at low potentials and coverage, molecules are weakly bound and can be swept over the surface by the tip. Further increase in potential to phase II (50 mV/SCE) leads to a more dramatic change in the surface/adlayer, as can be seen in Figure 3b. Most of the terraces now appear covered by organized structures divided into small domains, which will be referred as structure 1. The majority of these domains are formed by groups of 4−6 parallel lines, where the distance between lines amounts to about 1 nm. This film

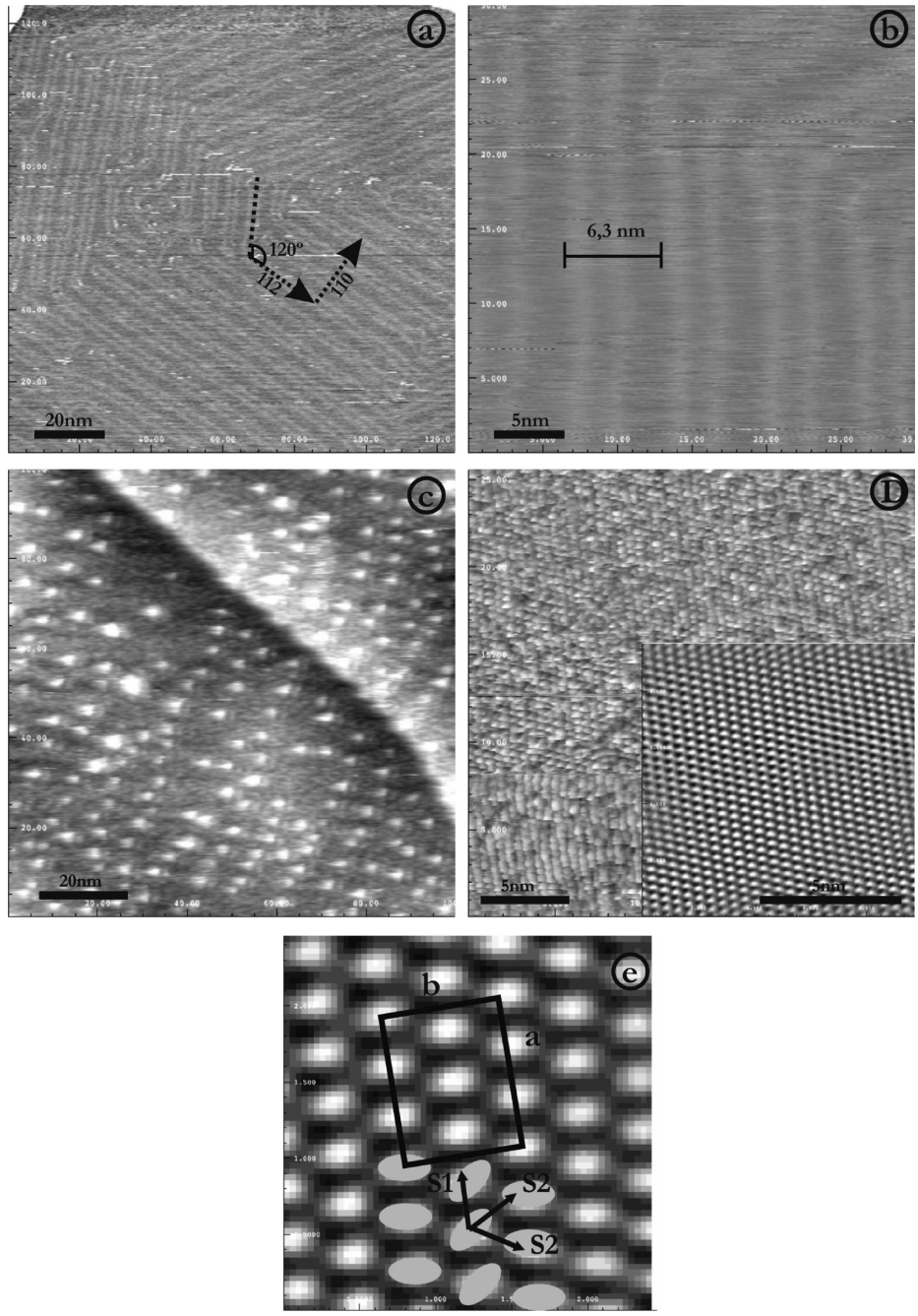

Figure 2. In situ STM images of the system 6 mM 5FU/50 mM H_2SO_4/Au(111) in the phases labeled in Figure 1. (a) Phase I: characteristic reconstruction pattern of Au(111) surface; $E_s = -100$ mV, $I_t = 5.5$ nA. (b) Phase II: no 2D pattern for the physisorbed 5FU; $E_s = 100$ mV, $I_t = 0.7$ nA. (c) Phase III: monatomic gold islands from the reconstruction lifting; $E_s = 450$ mV, $I_t = 1.1$ nA. (d) Phase IV: molecular resolution from the chemisorbed film; $E_s = 800$ mV, $I_t = 1$ nA; Inset: filtered and magnified image from (d). (e) Proposed model for phase IV: molecules (represented by ellipses) on adjacent rows are rotated with respect to each other. The arrows, labels, and bars were added to guide the eyes. All potentials are quoted relative to SCE.

shows a very high volatility: one single scan is enough to destroy the film. Higher resolution images for this single crystal in this phase could not be obtained. An examination of the directional behavior of the domains shows no evidence of an angular relationship between them. We could find domains whose main directions would form a variety of angles, not preferentially multiples of 60°. This lack of correlation with the underlying substrate symmetry indicates a weak interaction between substrate and adsorbate and implies that the molecule−molecule interaction is the dominant driving force responsible for the film stability. It is also relatively easy to resolve the lines, in contrast to the difficulty in resolving structures within the lines. This suggests that the 5FU molecules are forming directional bonds (1D), as opposed to 2D arrangements found for uracil (2D).[39] This kind of assembly resembles the one found for thymine when adsorbed on Au,[47] MoS_2, and HOPG.[22] A careful inspection of Figure 3b shows, at the upper right corner, a different structure which will be denoted as structure 2. It presents a similar structure, in the shape of long parallel lines, but the distances involved are much larger, about 1.8 nm. Increasing the surface potential to 100 mV/SCE (phase II) leads to a widespread dissolution of the structures 1 (not shown). The presence of the scanning tip may not be discarded as a major driving force for this dissolution. While domains with structure

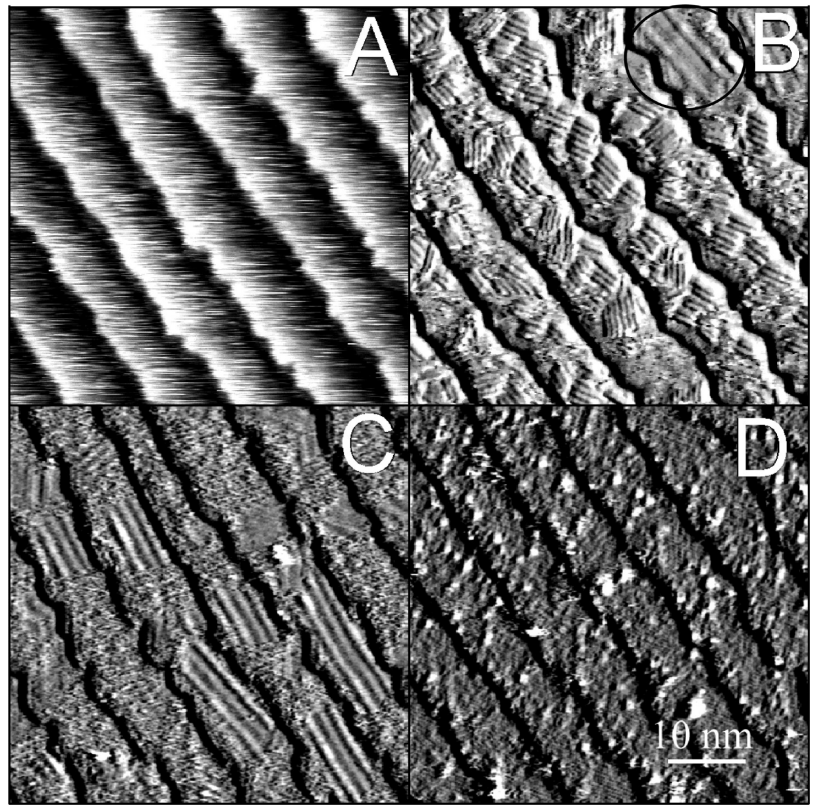

Figure 3. Potentiodynamic images followed by in situ STM of the system 6 mM 5FU/50 mM H_2SO_4/Au(111) from phase I to phase III: (a) $E_s = -40$ mV; (b) $E_s = 50$ mV; (c) $E_s = 350$ mV; (d) $E_s = 450$ mV; tunneling current, 1 nA. All potentials are quoted relative to SCE.

1 have almost completely vanished, new patches of structure 2 have appeared, but its coverage is very small. This type of image remains unchanged with the increase of potential up to roughly 300 mV/SCE. At 350 mV/SCE, near the threshold to phase III, structure 1 has totally disappeared, while structure 2 now covers a major portion of the surface, as can be seen in Figure 3c. This complex phase behavior shows the possibility of at least two metastable structures in this relatively large potential range. In fact, Hulme et al. have recently reported that solid 5FU crystals presents polymorphism,[50] so one would expect to have different patterns in the physisorbed flat-lying periodic structure. Unfortunately, this film is highly volatile avoiding higher resolution to be achieved. Finally, at 450 mV/SCE a new major surface change occurs: the lifting of surface reconstruction leading to gold island formation. In Figure 3d the gold islands can be clearly seen, although the molecules in this particular image are not resolved.

There is no consensus in the literature about the adsorption state of uracil in phase III. Figure 4 presents a series of low resolution STM images for a region with lower defect density (where we would expect the same features as in Figure 2). Figure 4a (phase I) is the same result discussed before: only substrate features (compare to Figure 2a). Further potential increase leads to the limits of phase II (300 mV/SCE), imaged in Figure 4b. Reconstruction lines are still present, but the grooves cannot be well-resolved like in Figure 4a, the surface becomes rougher and higher resolution is difficult to achieve (this is not electronic noise, once it was totally reproducible by alternating the surface potential from phase II to phase I and vice versa). We believe this is due to an increase of surface coverage of physisorbed 5FU molecules. Residence time of molecules on the surface is too short to be imaged, because the movement of the tip is slower than the adsorption dynamics. Further potential increase (Figure 4c, 350 mV/SCE) lifts the reconstruction in some regions at the right part of the image, as the lines disappear and gold islands are formed at the same place. This phenomenon is well characterized and follows the behavior for uracil:[39] the islands are smaller when compared to 5FU-free solution (not shown). Keeping the potential constant for longer times, the density of islands increases until reaching equilibrium, where reconstruction lines and gold islands coexist (Figure 4d). Scanning in a larger area (Figure 4e) shows that this phenomenon is restricted to the place where the tip was scanning, further corroborated when scanning at another region (Figure 4f), where the density of islands is lower. Only at 400 mV/SCE the reconstruction lines totally disappear.

These results show that probably the reconstruction lifting was tip-induced. In fact, this behavior has been reported in air[51] and in vacuum.[52] The images clearly show that reconstruction lifting at 350 mV/SCE is restricted to the vicinity of the step edges under the influence of STM tip. Determining whether the reconstruction lifting is due to surface charges or molecular adsorption is not straightforward because neither molecular resolution could be achieved nor the precise surface potential is known, because the local surface charge distribution is changed due to the tip presence. However, these observations are in agreement with previous studies of tip-induced phase transitions[51,52] and support the idea of a nucleation starting at step edges.

Back to the discussion of molecular adsorption in phase II, the STM results show distinct behavior for different morphologies (large terraces or stepped surfaces). As the defect density increases, more sites for heterogeneous nucleation become available. In much smaller terraces, a few molecular units wide, the energetics of the step edge help stabilize the film allowing its imaging by STM. In our measurements the average width of a terrace is about 8 nm which is in good agreement with the estimation of the minimum size of a terrace for transition I↔II

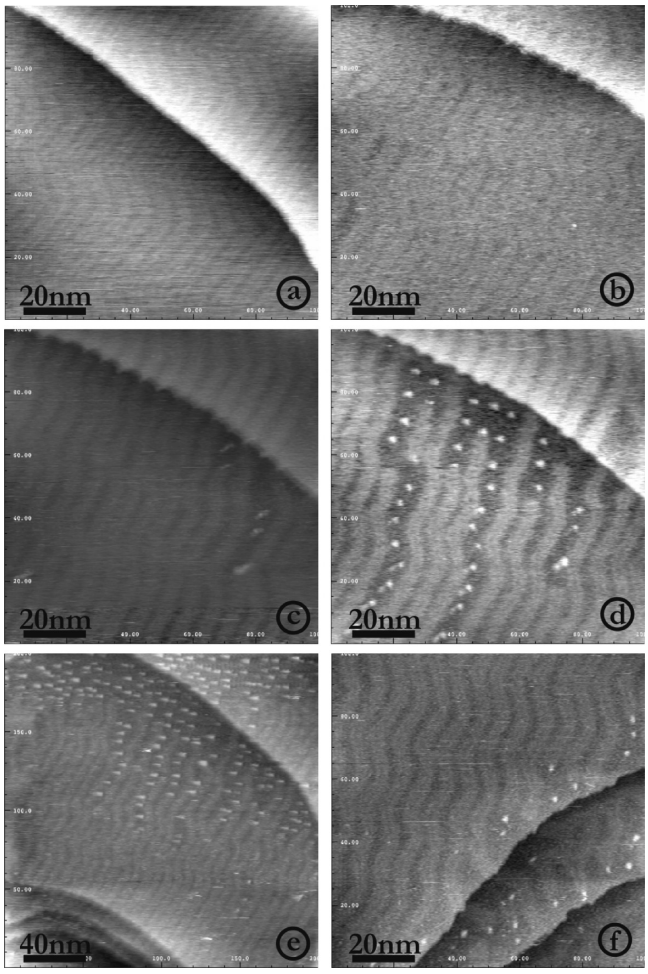

Figure 4. Potentiodynamic images followed by in situ STM of the system 6 mM 5FU/50 mM H_2SO_4/Au(111) from phase I to the borderline of phases II and III: (a) $E_s = -100$ mV; (b) $E_s = 300$ mV; (c) $E_s = 350$ mV, $t = 0$ s; (d) $E_s = 350$ mV, $t = 3$ min; (e) $E_s = 350$ mV, after $t = 150$ min; and (f) $E_s = 350$ mV, $t = 150$ min, but at a different location. Tunneling currents range from 0.06−1.6 nA. All potentials are quoted relative to SCE.

to be detected by CV technique (28 atoms or about 8 nm).[43] As one can see from the results on large terraces (Figure 2b), no adsorbate periodic patterns could be imaged, further corroborating this interpretation. Because an imperfect surface is necessary for the formation of this highly volatile film, we propose that there is only an increase in the surface population of 5FU in phase II, but it does not form any periodic pattern like the ones commonly observed for physisorbed films of uracil and thymine. Further studies using stepped surfaces should help clarify this question and will be pursued in the near future.

Remarks on Halogen Uracil Adsorption Behavior. Both physisorbed and chemisorbed states 5FU presented unusual behavior compared to other uracil derivatives. The first issue we want to address is the reason for 5FU not forming any periodic structure upon physisorption in phase II (considering an ideal (111) flat surface). It is known that methyl groups in N1 or N3 position blocks the sites for hydrogen bonding and no 2D physisorbed periodic structure is formed.[19] Comparison among solid crystal structures of uracil derivatives show that they form planar layers stabilized by hydrogen bonds within the layers using the N3 site.[17,49,53−55] A possible answer to the question above may be obtained by combining recent molecular dynamic studies on the early stages of crystal structure formation with the effect of incorporating 5FU into DNA/RNA helix: (*i*) 5FU incorporation into DNA turns it into a less stable structure, leading to base mismatch;[56] (*ii*) a molecular dynamics study has shown that the growth mechanism for the crystal structure is distinctly different when water or nitromethane is the solvent, and water strongly hydrogen bonds to 5FU;[57] (*iii*) moreover, stacked structures are preferred instead of dimers formation (5FU-5FU) by hydrogen bonding.[58] Therefore, we can argue that the presence of halogen in the pyrimidine ring enhances π-stacking. Thus, in phase I, water and 5FU molecules are randomly physisorbed and probably 5FU is stabilized by water hydrogen bonds, not by surrounding 5FU molecules. Further potential increase to phase II does not disrupt the 5FU−water interaction, so that 5FU−5FU hydrogen bonds are not preferred, but perhaps stacked structures may result.

One can argue about the different behavior between molecules in solution and under the action of intense electric fields at the solid/solution interface. STM results with 5ClU and 5BrU in phase II show that only 5BrU forms a flat-lying periodic structure (for 5ClU is proposed an *upstanding position*), in good agreement with X-ray crystallographic data.[55] Because the crystals of these two molecules (5ClU and 5BrU) are nearly isostructural, it is expected they both would form 2D flat-lying periodic structure, however, 5ClU does not. Ab initio calculations of hydrogen bond distances in base pairing[7] show that there is a shortening trend as follows: |5FU−adenine| = |5ClU−adenine| > |5BrU−adenine| > |uracil−adenine| (the hydrogen bonding between complementary pairs in the Watson−Crick structure is made through the N3 position). Because shorter hydrogen bonds tend to be stronger[59] and assuming that the uracil derivatives with stronger hydrogen bonds at the N3 site tend to associate among themselves in planar structures, this trend, evaluated by ab initio calculations, indicates that the tendency to form 2D flat-lying periodic structures for the halogen uracils at Au(111) electrified interface should follow this sequence: 5FU = 5ClU < 5BrU < U.[47] This is indeed observed by STM images: neither 5FU nor 5ClU forms 2D flat-lying periodic structures, but 5BrU and uracil do.

The second issue to address is the reason why 5FU has such a high surface coverage upon chemisorption (phase IV). Table 1 shows the area per molecule for uracil derivatives from STM results and interlayer distances from solid crystal structure. It

TABLE 1: Crystal Interlayer and Adlayer Parameters for Uracil Derivatives

molecule	crystal interlayer distance[a] (Å)	adsorbate−adsorbate distance[b] (Å)	area/molecule (Å^2)
thymine	3.36	4.9[d]	28
uracil	3.34	4.9	21
5-bromouracil	3.4		
5-clorouracil	3.3	3.4	18
5-fluorouracil	2.96−3.27[c]	3.3	14

[a] From refs 54, 53, 55, and 49, respectively. [b] These are distances in the direction of closest approach (the molecules could be rotated). [c] It was not given any average value. [d] Taken from the ordered domains.

is expected that the substitution of a hydrogen in uracil by a methyl group (thymine) leads to steric repulsion, so intermolecular distances increase, enlarging the area occupied by the molecule (compare uracil and thymine) upon chemisorption. Substitution of a hydrogen in uracil by fluorine in 5FU should keep approximately the same intermolecular distance between layers of molecules in the solid crystal structure, but this is not observed upon chemisorption. The same behavior is observed in 5ClU adlayers: shorter molecular distance when compared to uracil. What we can learn from these images and crystal data comparison is that the halogenation in 5-position enhances π-stacking between molecules. This tendency tells us that halogenation of uracil enhances adsorbate−adsorbate with respect to adsorbate−substrate interactions. In fact the incorporation of halogen uracil decreases the stability of DNA/RNA, probably due to stronger dispersive forces along the chain and weakening of the hydrogen-bonding through the N3 site.[56]

The assumption that each spot in Figure 2d is a single 5FU molecule rather than a mixed system of 5FU/water coadsorption[46] is corroborated by the decreasing area occupied by the derivatives following the size of the halogen.

Conclusions

We have studied the behavior of 5FU adsorbed at the Au(111) electrified interface and compared to other uracil derivatives. Four distinct phases were resolved. In negative electrode potentials the molecules are randomly physisorbed (phase I). In phase II, opposite to uracil, no physisorbed periodic structure could be characterized on flat surfaces, but only an increase in surface population. This was explained in terms of enhanced π-stacking between 5FU molecules and hydrogen bonding sites blocked by water molecules. For a high defect density surface, a periodic pattern could be imaged in phase II, probably stabilized by high-energy adsorption sites. Phase III is characterized by tip-induced reconstruction lifting of the gold surface, forming monatomic gold islands on the surface which are stabilized by adsorbed 5FU molecules. In positive potentials, (phase IV) molecular resolution could be achieved for an ordered upstanding chemisorbed structure with the highest density reported for pyrimidine derivatives on Au(111).

Comparisons with available data in the literature have shown that the surface coverage follows the same tendency for crystal structures: π-stacking is enhanced when halogens are incorporated in the uracil structure, which increases the molecular density upon chemisorption. This understanding of the delicate balance of H-bonding and π-stacking interactions in determining the final structure of adsorbates is important in many areas of surface science and could eventually allow a molecular design of adlayers to enhance surface stability or increase coverage, among other properties.

Acknowledgment. H.B.d.A. thanks Janete Giz for assistance in STM operation, Kleber Bergamaski, Janaina Gomes, and Vinicius Delcolle for helping with electrochemical experiments, Ana Paula Camargo for reading the manuscript, Ines Moraes for CV measurements, and CAPES for financial support. This work was supported by the Brazilian agencies CNPq, FAPESP, and FINEP.

Supporting Information Available: Additional CV experiments in a high defect-density single crystal and STM images of phase II on low defect-density single crystal (large (111) terraces) under very low tunneling currents. This material is available free of charge via the Internet at http://pubs.acs.org.

References and Notes

(1) Kubota, M.; Kobayashi, T. *J. Electron Spectrosc. Relat. Phenom.* **1996**, *82*, 61.
(2) Gustavsson, T.; Bányáz, Á.; Lazzarotto, E.; Markovits, D.; Scalmani, G.; Frisch, M. J.; Barone, V.; Improta, R. *J. Am. Chem. Soc.* **2005**, *128*, 607.
(3) Nguyen, M. T.; Zhang, R.; Nam, P. C.; Ceulemans, A. *J. Phys. Chem. A* **2004**, *108*, 6554.
(4) Muller, A.; Leutwyler, S. *J. Phys. Chem. A* **2004**, *108*, 6156.
(5) Orozco, M.; Hernández, B.; Luque, F. J. *J. Phys. Chem. B* **1998**, *102*, 5228.
(6) Yekeler, H.; Özbakir, D. *J. Mol. Model.* **2001**, *7*, 103.
(7) Yang, Z.; Rodgers, M. T. *J. Am. Chem. Soc.* **2004**, *126*, 16217.
(8) Freese, E. *J. Mol. Biol.* **1959**, *1*, 87.
(9) Poon, M. A.; O'Connell, M. J.; Moertel, C. G.; Wieand, H. S.; Cullinan, S. A.; Everson, L. K.; Krook, J. E.; Mailliard, J. A.; Laurie, J. A.; Tschetter, L. K. *J. Clin. Oncol.* **1989**, *7*, 1407.
(10) Lopez, A.; Chen, Q.; Richardson, N. V. *Surf. Interface Anal.* **2002**, *33*, 441.
(11) Paciotti, G. F.; Myer, L.; Weinreich, D.; Goia, D.; Pavel, N.; McLaughlin, R. E.; Tamarkin, L. *Drug Delivery* **2004**, *11*, 169.
(12) Sowerby, S. J.; Stockwell, P. A.; Heckl, W. M.; Petersen, G. B. *Origins Life Evol. Biosphere* **2000**, *30*, 81.
(13) Heckl, W. M.; Smith, D. P. E.; Bining, G.; Klagges, H.; Hänsch, T. W.; Maddocks, J. *Proc. Natl. Acad. Sci. U.S.A.* **1991**, *88*, 8003.
(14) DeLevie, R. *Chem. Rev.* **1998**, *88*, 599.
(15) Buess-Herman, C. *Prog. Surf. Sci.* **1994**, *46*, 335.
(16) Baker, J. G.; Cristian, S. D.; Kim, M. H.; Dryhurst, G. *Byophys. Chem.* **1979**, *9*, 355.
(17) De Levie, R.; Wandlowski, Th. *J. Electroanal. Chem.* **1994**, *366*, 265.
(18) Lipkowski, J., Ross, P. N., Eds. *Adsorption of molecules at metal electrodes*; VCH: New York, 1992.
(19) Wandlowski, T.; Hölzle, M. H. *Langmuir* **1996**, *12*, 6604.
(20) Wandlowski, T. *J. Electroanal. Chem.* **1995**, *395*, 83.
(21) Hölzle, M. H.; Wandlowski, T.; Kolb, D. M. *Surf. Sci.* **1995**, 335.
(22) Sowerby, S. J.; Petersen, G. B. *J. Electroanal. Chem.* **1997**, *433*, 85.
(23) Tao, N. J.; DeRose, J. A.; Lindsay, S. M. *J. Phys. Chem.* **1993**, *97*, 910.
(24) Cavallini, M.; Aloisi, G.; Bracali, M.; Guidelli, R. *J. Electroanal. Chem.* **1998**, *444*, 75.
(25) Kawai, T.; Tanaka, H.; Nakagawa, T. *Surf. Sci.* **1997**, *386*, 124.
(26) Mamdouh, W.; Dong, M.; Xu, S.; Rauls, E.; Besenbacher, F. *J. Am. Chem. Soc.* **2006**, *128*, 13305.
(27) Camargo, A. P. M.; Baumgärtel, H.; Donner, C. *Phys. Chem. Chem. Phys.* **2003**, *5*, 1657.
(28) Xu, S.; Dong, M.; Rauls, E.; Otero, R.; Linderoth, T. R.; Besenbacher, F. *Nano Lett.* **2006**, *6*, 1434.
(29) Kirste, S.; Donner, C. *Phys. Chem. Chem. Phys.* **2001**, *3*, 4384.
(30) Screiber, F. *Prog. Surf. Sci.* **2000**, *65*, 151.
(31) Cunha, F.; Tao, N. J. *Phys. Rev. Lett.* **1995**, *75*, 2376.
(32) Su, G. J.; Zhang, H. M.; Wan, L. J.; Bai, C. L. *Surf. Sci.* **2003**, *531*, L363.
(33) Petsalakis, I. D.; Theodorakopoulos, G. *Israel J. Chem.* **2005**, *45*, 127.
(34) Meyerheim, H. L.; Gloege, Th. *Chem. Phys. Lett.* **2000**, *326*, 45.
(35) Cao, Y.; Deng, J. F.; Xu, G. Q. *J. Chem. Phys.* **2000**, *112*, 4759.
(36) Cunha, F.; Sá, E.; Nart, F. *Surf. Sci.* **2001**, *480*, L383.
(37) Wandlowski, T.; Kretschmer, E.; Müller, E.; Kuschel, F.; Hoffmann, S.; von Lipinski, K. J. *J. Electroanal. Chem.* **1986**, *213*, 339.
(38) Meyerheim, H. L.; Maltor, H.; Robinson, I. K. *Chem. Phys. Lett.* **2003**, *326*, 45.
(39) Dretschkow, Th.; Dakkouri, A. S.; Wandlowski, T. *Langmuir* **1997**, *13*, 2843.
(40) Dretschkow, T.; Wandlowski, T. *Ber. Bunsen-Ges. Phys. Chem.* **1997**, *101*, 749.
(41) Baré, S.; Van krieken, M.; Buess-Herman, C.; Hamelin, A. *J. Electroanal. Chem.* **1998**, *445*, 7.
(42) Wandlowski, Th.; Ataka, K.; Pronkin, S.; Diesing, D. *Electrochim. Acta* **2004**, *49*, 1233.
(43) Pronkin, S.; Wandlowski, Th. *J. Electroanal. Chem.* **2003**, *550*, 131.
(44) Guerrieri, A.; Cataldi, T. R. I.; Palmisano, F.; Zambonin, P. G. *J. Electroanal. Chem.* **1991**, *314*, 117.
(45) Kolb, D. M. *Prog. Surf. Sci.* **1996**, *51*, 109.
(46) Roefls, B.; Bunge, E.; Schröter, C.; Solomun, T.; Meyer, H.; Nichols, R. J.; Baumgärtel, H. *J. Phys. Chem. B* **1997**, *101*, 754.
(47) Cunha, F. G. C. Ph.D. Thesis, Universidade de São Paulo, Instituto de Química de São Carlos, Brazil, 2001.
(48) Li, W. H.; Haiss, W.; Floate, S.; Nichols, R. J. *Langmuir* **1999**, *15*, 4875.

(49) Fallon, L., III. *Acta Crystallogr. B* **1973**, *29*, 2549.
(50) Hulme, A. T.; Price, S. L.; Tocher, D. A. *J. Am. Chem. Soc.* **2005**, *127*, 1116.
(51) Schott, J. H.; White, H. S. *Langmuir* **1998**, *8*, 1955.
(52) Buisset, J.; Rust, H.-P.; Schweizer, E. K.; Cramer, L.; Bradshaw, A. M. *J. Vac. Sci. Technol. B* **1996**, *14*, 1117.
(53) Parry, G. S. *Acta Crystallogr.* **1954**, *7*, 313.
(54) Ozeki, K.; Sakabe, N.; Tanaka, J. *Acta Crystallogr.* **1969**, *B25*, 1038.
(55) Sternglanz, H.; Bugg, C. E. *Biochem. Biophys. Acta* **1975**, *378*, 1.
(56) Kremer, A. B.; Mikita, T.; Beardsley, G. C. *Biochemistry* **1987**, *26*, 391.
(57) Hamad, S.; Moon, C.; Catlow, C. R. A.; Hulme, A. T.; Price, S. L. *J. Phys. Chem. B* **2006**, *110*, 3323.
(58) Alagona, G.; Ghio, C.; Monti, S. *Int. J. Quantum Chem.* **2002**, *88*, 133.
(59) Jeffrey, G. A. *An Introduction to Hydrogen Bonding*; Oxford University Press: Oxford, 1991.

JP100890A

Supporting Information for the article "Adsorption Behavior of 5-fluorouracil on Au (111): an *in-situ* STM Study"

H. B. de Aguiar,[1,♦] F. G. C. Cunha,[3] F. C. Nart[2,†] and P. B. Miranda[1,*]

[1]Instituto de Física de São Carlos and [2]Instituto de Química de São Carlos, Universidade de São Paulo, CP 369, São Carlos, São Paulo, Brazil, 13560-970

[3]Departamento de Física, Universidade Federal de Sergipe, CP 353, São Cristóvão, Sergipe, Brazil, 49100-000

In this supplementary information we added extra CV experiments in a high defect-density single crystal and STM images of low defect-density single crystal (large (111) terraces) in phase II under very low tunneling currents.

♦ current address: Max-Planck-Institute für Metallforschung, Heisenbergstrasse 3, 70569, Stuttgart, Germany.
† Deceased. We dedicate this work to his memory.
* Corresponding author. e-mail: miranda@ifsc.usp.br

CV of a high defect-density Au(111) single crystal

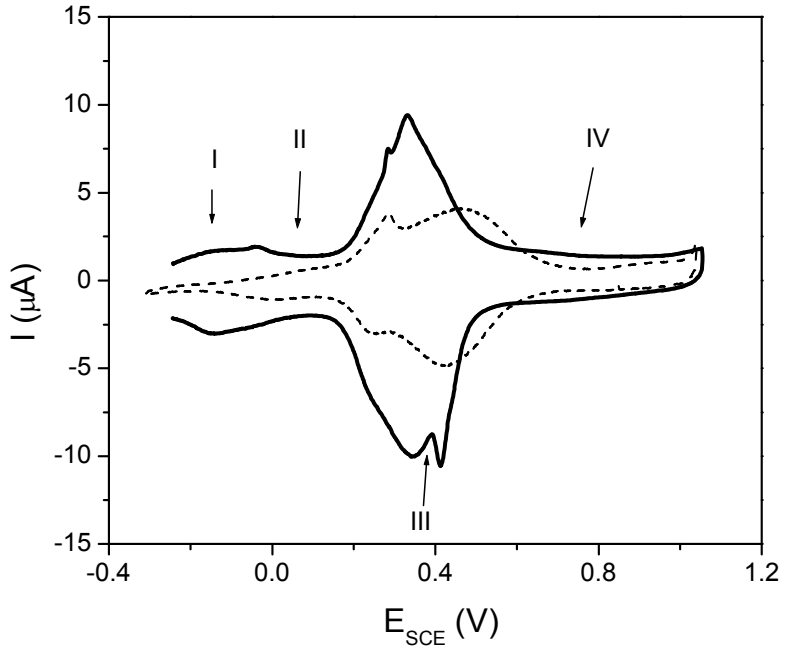

Figure S1. Steady state cyclic voltammogram of the system 6 mM 5FU/50 mM H_2SO_4 /Au(111). Scan rate 50 mVs^{-1}. Continuous lines are with 5FU and dashed without 5FU. This single crystal presents a higher defect density compared to the one present in Figure 1.

Figure S1 presents a steady state CV of a high defect-density single crystal of the systems 6 mM 5FU/50 mM H_2SO_4/Au(111) and 5FU-free (dashed lines). The phase transitions peaks are broaden due to the high defect-density of this single-crystal.[1] The sharp current peak of the transition I↔II could not be detected but just a broad feature circa - 40 mV/SCE. Further potential increase leads to a broad current peak centered at 330 mV/SCE superimposed on a sharp one at ~ 280 mV/SCE, which we assign to phase transitions between phases III-IV and phases II-III, respectively. Even at the highest bulk concentration (up to 36 mM) no spike in the CV could be resolved.

The 5FU-free CV (dashed lines in Figure S1) shows the characteristic features expected for this system. The peak at ~ 280 mV/SCE is due to the reconstruction lifting. The absence of a sharp peak at ~ 800 mV/SCE of disorder/order sulfate adlayer phase transition, which is sensitive to the amount of defect density,[12] corroborates the assignment of a high defect-density single crystal

STM images with low tunneling current

In Figure S2, STM images of the system 18 mM 5FU/50 mM H_2SO_4/Au(111) are presented. All the images are within substrate potentials of the phase II. If there were a 2D flat-flying periodic structure, features with a periodicity approximately 0.7 nm could be imaged characteristic of uracil derivative adlayers on Au(111).[3] However, only the substrate lattice could be imaged, even with the lowest achievable tunneling current (66 pA). In Figure S2a the reconstruction lines of the Au(111) can be clearly seen with regions with high level of noise and regions showing some periodic pattern. Figure S2b is the zoomed in and filtered region of the periodic pattern of Figure S2a. The periodicity is the same of the Au-Au distance (0.27 nm) indicating that we are imaging the substrate (111) lattice. In Figure S2c, the image was taken after sweeping the potential from phase IV to phase II, with the tip relocated and raised for ca. 30 min and then imaging started. Even though in this scheme we had a lower noise level, it was not possible to image the ordered adlayer at any resolution level but only the substrate lattice at atomic resolution.

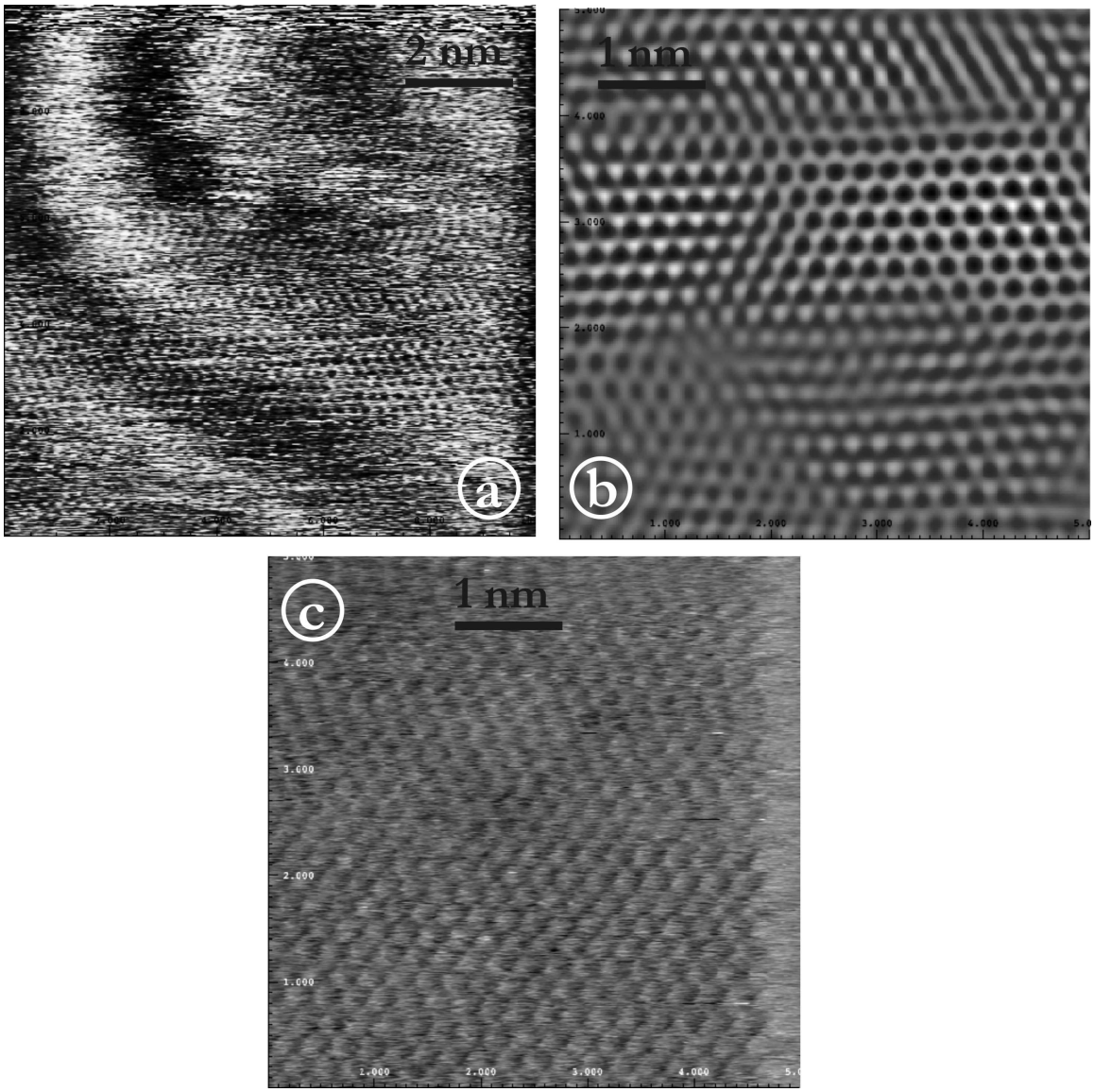

Figure S2. *In-situ* STM images of the system 18 mM 5FU/50 mM H_2SO_4/Au(111). a) E_s = 100 mV, I_t = 66 pA. b) zoomed in and filtered image from a). c) E_s = 150 mV, I_t = 0,72 nA. All potentials are quoted relative to SCE.

References

[1] Pronkin, S.; Wandlowski, Th. *J. Electroanal. Chem.* **2003**, *550*, 131;
[2] Wandlowski, Th.; Ataka, K.; Pronkin, S.; Diesing, D. *Electrochim. Acta* **2004**, *49*, 1233;
[3] Dretschkow, Th.; Dakkouri, A. S.; Wandlowski, T. *Langmuir* **1997**, *13*, 2843; Cunha, F. G. C. *Ph.D. Thesis*, Universidade de São Paulo, Instituto de Química de São Carlos, Brazil, 2001.